

# Pruning the Pilots: Deep Learning-Based Pilot Design and Channel Estimation for MIMO-OFDM Systems

Mahdi Boloursaz Mashhadi and Deniz Gündüz

Dept. of Electrical and Electronic Eng., Imperial College London, UK

Email: {m.boloursaz-mashhadi, d.gunduz}@imperial.ac.uk

## Abstract

With the large number of antennas and subcarriers, the overhead due to pilot transmission for channel estimation can be prohibitive in wideband massive multiple-input multiple-output (MIMO) systems. This can degrade the overall spectral efficiency significantly, and curtail the potential benefits of massive MIMO. In this paper, we propose a deep neural network (DNN)-based scheme, consisting of convolutional and dense layers, for joint pilot design and downlink channel estimation for frequency division duplex (FDD) MIMO orthogonal frequency division duplex (OFDM) systems. We also propose an effective pilot reduction technique by gradually pruning less significant neurons from the dense neural network (NN) layers during training. Our proposed NN-based scheme exploits the frequency-specific features of the propagation environment to design more efficient pilots. It outperforms linear minimum mean square error (LMMSE) estimation by learning the channel statistics over the training data and exploiting it to estimate the channel without prior assumptions on the channel distribution. Finally, our pruning-based pilot reduction technique effectively reduces the overhead by allocating pilots across subcarriers non-uniformly; allowing less pilot transmissions on subcarriers that can be satisfactorily reconstructed by the subsequent convolutional layers utilizing inter-frequency correlations.

## I. INTRODUCTION

Massive multiple-input multiple-output (MIMO) systems are considered as the main enabler of 5G and future wireless networks thanks to their ability to serve a large number of users simultaneously, achieving impressive levels of spectral efficiency. A base station (BS) with a massive number of antennas relies on accurate downlink channel state information (CSI) to

achieve the promised performance gains. Therefore, massive MIMO systems are more amenable to time division duplex (TDD) operation, which, thanks to the reciprocity of the uplink and downlink channels, does not require downlink channel estimation at the users. FDD operation more is more desirable due its improved coverage and reduced interference; however, channel reciprocity does not hold in FDD. In FDD MIMO, the BS broadcasts downlink pilot signals, the users estimate the channel from the received pilots and transmit the CSI feedback to the BS. The resulting feedback overhead becomes significant due to the large number of antennas and users; and hence, efficient pilot design and channel estimation are crucial to reduce the overhead.

In massive MIMO systems the pilot length is typically much smaller than the number of antennas, channel estimation becomes severely underdetermined where simple least squares (LS) channel estimation and orthogonal FFT pilots become obsolete. On the other hand, the popular linear minimum mean square error (LMMSE) technique is based on the Gaussian channel assumption and requires the channel covariance matrix. In practice, channel distributions may deviate from Gaussian and covariance matrices need to be estimated from the received signals at the user which degrades the LMMSE performance.

To estimate the channel more efficiently and reduce the pilot overhead, many previous works take a model-based estimation approach assuming sparse [1]–[5] or low-rank [6], [7] models on the channel matrix and utilize compressive sensing (CS)-based reconstruction techniques to estimate the channel or design improved pilot sequences. CS-based approaches rely on sparse or low-rank properties of the channel, which may not represent the channel structure accurately for many practical MIMO scenarios. CS-based approaches do not take into account the inherent statistical correlations and structures beyond sparse or low-rank patterns. Moreover, CS-based reconstruction techniques employ computationally demanding iterative algorithms, which imposes an additional burden considering the limited computational resources available at the users.

More recently, deep learning (DL)-based approaches have been used for massive MIMO channel state (CSI) acquisition and showed significant improvements in comparison with their counterparts based on sparsity and compressive sensing (refer to [8], [9], and references therein). In these works, deep neural network (DNN) architectures are trained over large CSI datasets to learn complex CSI distributions, structures and correlations and exploit them for data-driven pilot design [10], channel estimation [11]–[15], compression [16]–[21] and feedback [22], [23] tasks. Many of these works focus on a single task and propose a NN architecture to achieve optimized

performance for it. However, MIMO CSI acquisition involves all the mentioned tasks. Although designing a single NN architecture to simultaneously handle all or several of these tasks is desirable for an end-to-end optimized performance, the resulting NN involves a more challenging training process with its increased number of parameters. In this research, we consider joint pilot design and channel estimation for downlink FDD massive MIMO systems.

In [11], [24], the authors proposed a convolutional neural network (CNN)-based structure for massive MIMO channel estimation. Their proposed architecture outperforms non-ideal LMMSE-based channel estimation (where the required covariance matrices are estimated from a coarse initial estimate of the channel at the receiver) and approach ideal LMMSE (with perfect knowledge of covariance matrices assumed at the receiver). In [10], the authors use dense layers (which represent the pilots) followed by subsequent convolutional layers for joint pilot design and channel estimation. However, they design the same pilots for all subcarriers which not only neglects frequency specific features in the CSI, but also results in a large PAPR which is practically undesirable.

In this work we propose a DNN-based scheme consisting of convolutional and dense layers for downlink pilot design and channel estimation in FDD massive MIMO-OFDM systems. Our proposed NN-based scheme exploits frequency-specific features for more efficient pilot design and channel estimation. Our proposed architecture learns channel statistics over a dataset during training and exploits it to design pilots and estimate the channel without requiring covariance matrices or other prior statistical assumptions. Our structure improves the normalized mean square error (NMSE) in comparison with [11], [24], and outperforms the ideal linear minimum mean square error (LMMSE) estimation thanks to our frequency-aware pilot design layers. In comparison with [10], we use a frequency-aware pilot design scheme which outperforms simple frequency-independent pilot design in [10] by a large margin. Frequency-aware pilot design also enables us to allocate pilots non-uniformly over different subcarriers by our proposed pilot reduction technique based on NN pruning. Our pruning-based pilot reduction technique effectively reduces pilot overhead by allocating pilots across subcarriers non-uniformly; fewer pilots are transmitted on subcarriers that can be satisfactorily reconstructed by the subsequent convolutional layers utilizing inter-frequency correlations.

This paper is organized as follows. In Section II, we present the system model. In Section III we present the proposed DNN architecture for joint pilot design and channel estimation. In section IV we present our pilot reduction scheme by NN pruning. Section V provides the

simulation results, and Section VI concludes the paper.

## II. SYSTEM MODEL

We consider an FDD massive MIMO system, where a BS with  $N$  antennas serves a single-antenna user utilizing orthogonal frequency division multiplexing (OFDM) over  $M$  subcarriers. We denote the downlink channel by  $\mathbf{H} = [\mathbf{h}_1, \mathbf{h}_2, \dots, \mathbf{h}_M] \in \mathbb{C}^{N \times M}$ , where  $\mathbf{h}_m \in \mathbb{C}^N$  is the channel gain vector over subcarrier  $m$ , for  $m = 1, \dots, M$ . We assume that the BS is equipped with a uniform linear array (ULA) with response vector:

$$\mathbf{a}(\phi) = [1, e^{-j\frac{2\pi d}{\lambda} \sin \phi}, \dots, e^{-j\frac{2\pi d}{\lambda} (N-1) \sin \phi}]^T / \sqrt{N},$$

where  $\phi$  is the angle of departure (AoD), and  $d$  and  $\lambda$  denote the distance between adjacent antennas and carrier wavelength, respectively. The channel gain is a summation of multipath components given by

$$\mathbf{h}_m = \sqrt{\frac{N}{L}} \sum_{l=1}^L \alpha_l e^{-j2\pi\tau_l f_s \frac{m}{M}} \mathbf{a}(\phi), \quad (1)$$

where  $L$  is the number of multipath components,  $f_s$  is the sampling rate,  $\tau_l$  is the delay, and  $\alpha_l$  is the propagation gain of the  $l^{\text{th}}$  path. According to Eq. (1), entries of the channel matrix  $\mathbf{H}$  are correlated for nearby sub-carriers and antennas due to similar propagation paths, gains, and AoDs/AoAs. There also exists inherent characteristics in MIMO environments due to specific user distributions, scattering parameters, geometry, etc., that cause common structures among MIMO channel matrices.

Denoting downlink pilot signals transmitted by the BS over the  $m^{\text{th}}$  subcarrier by  $\mathbf{P}_m \in \mathbb{C}^{L \times N}$ , where  $L$  is the pilot length, the received signal at the user is given by

$$\mathbf{y}_m = \mathbf{P}_m \mathbf{h}_m + \mathbf{n}_m, \quad (2)$$

where  $\mathbf{n}_m \sim \mathcal{CN}(0, \sigma^2)$  is the complex additive Gaussian noise over the  $m^{\text{th}}$  subcarrier, which is independent across subcarriers. We propose a DNN architecture to jointly design the optimum pilot signals  $\mathbf{P}_1, \dots, \mathbf{P}_M \in \mathbb{C}^{L \times N}$  and estimate the downlink channel matrix  $\mathbf{H}$  from the signals received at the user over all subcarriers, i.e.,  $\mathbf{Y} = [\mathbf{y}_1, \mathbf{y}_2, \dots, \mathbf{y}_M]^T \in \mathbb{C}^{M \times L}$ . A large pilot length  $L$  is infeasible not only because it increases the training overhead and computational complexity for channel estimation, but also because  $L$  should be much smaller than the channel coherence interval. Hence, in massive MIMO systems, where  $N$  is excessively large, the pilot length  $L$  is typically much smaller than the number of antennas  $N$  and Eq. (2) is severely underdetermined.

Standard channel estimation techniques are typically based on linear minimum mean square error (LMMSE) estimation method where the pilot signals are orthogonal discrete cosine transform (DFT) basis vectors or Zadoff-Chu sequences. The LMMSE channel estimate is based on Gaussian channel assumption and requires the knowledge of channel and noise covariance matrices. In practical MIMO scenarios, the channel statistics may deviate from Gaussian and the covariance matrices need to be empirically estimated from the received signal at the user, which degrades the LMMSE performance. On the other hand, the simple choice of orthonormal DFT or Zadoff-Chu pilot signals regardless of the specific medium characteristics, e.g., scatterer positions, environment geometry, carrier frequencies, etc., is sub-optimal as will be discussed further in the next section. On the other hand the LMMSE estimator neglects inherent structures in typical MIMO channel matrices according to Eq. (1), but these structures can be exploited to further improve the estimation performance.

NNs are extremely powerful tools in learning complex distributions which motivates the use of NN-based data-driven approaches for channel estimation and pilot design in massive MIMO. Our proposed approach utilizes a NN architecture for joint channel estimation and pilot design without prior assumptions on distributions or statistics. The NN learns the required distributions, correlations and statistics over the dataset during training and leverage them for efficient channel estimation and pilot design thereby reducing the overhead.

### III. THE PROPOSED APPROACH

Fig. 1 depicts our proposed NN architecture for data-driven channel estimation and frequency-aware pilot design, where double-channel inputs and outputs represent real and imaginary parts of the corresponding channel matrices. The network is composed of  $M$  fully connected branches, one for each subcarrier, followed by 3 convolutional layers, and is trained end-to-end to minimize the mean square error (MSE). Each branch is composed of 2 dense layers, a reduction and an expansion layer denoted by  $\mathcal{FC}^r$  and  $\mathcal{FC}^e$ , respectively.

The input CSI matrix  $\mathbf{H}$  is first divided into its subcarrier components  $\mathbf{h}_1, \mathbf{h}_2, \dots, \mathbf{h}_M$ , where  $\mathbf{h}_m$  is input to the  $m$ 'th fully connected branch. The reduction layer in each branch models downlink pilot transmission over that subcarrier, which is followed by downlink additive Gaussian noise according to  $\mathbf{y}_m = \mathcal{FC}_m^r(\mathbf{h}_m; \mathbf{P}_m) + \mathbf{n}_m = \mathbf{P}_m \mathbf{h}_m + \mathbf{n}_m$ . Hence, the weight parameters trained for  $\mathcal{FC}_m^r$  correspond to the pilots to be transmitted over the  $m$ 'th subcarrier, denoted by

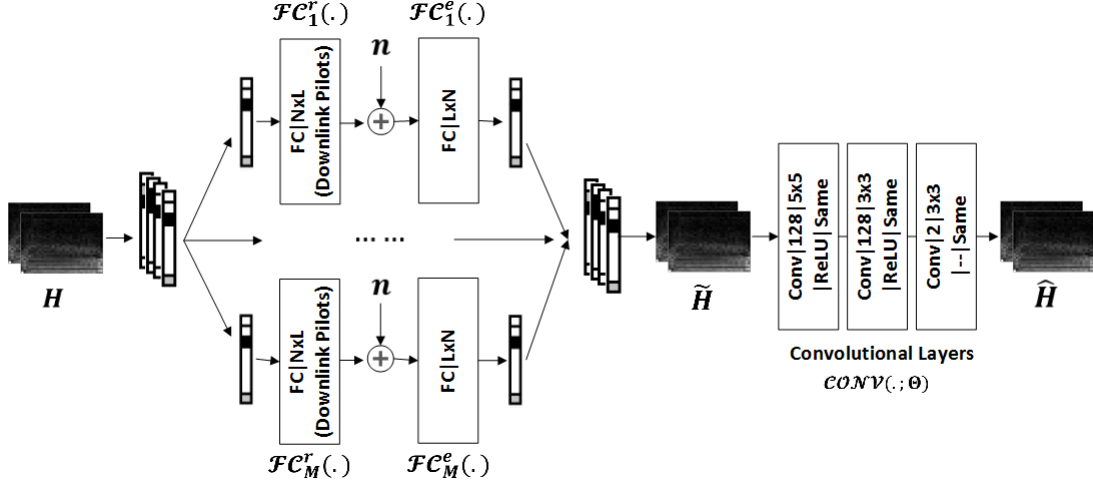


Fig. 1: Block diagram of the proposed scheme.

$\mathbf{P}_m^*$ . Note that the dense layers  $\mathcal{F}C_1^r, \dots, \mathcal{F}C_M^r$  are used without bias or activations here, as they imitate the actual pilot transmission process, which is a simple matrix multiplication.

The expansion layer in the  $m$ 'th branch gives a coarse initial estimate of the channel at  $m$ 'th subcarrier according to  $\tilde{\mathbf{h}}_m = \mathcal{F}C_m^e(\mathbf{y}_m; \mathbf{Q}_m, \mathbf{b}_m) = \mathbf{Q}_m \mathbf{y}_m + \mathbf{b}_m$ . This initial estimate imitates the familiar LMMSE estimate  $\hat{\mathbf{h}}_m^{MMSE} = \mathbb{E}[\mathbf{h}_m] + \mathbf{R}_{h_m y_m} \mathbf{R}_{y_m y_m}^{-1} (\mathbf{y}_m - \mathbb{E}[\mathbf{y}_m])$ , where  $\mathbb{E}[\mathbf{h}_m]$  and  $\mathbb{E}[\mathbf{y}_m]$  are the corresponding expected values, and  $\mathbf{R}_{h_m y_m}$  and  $\mathbf{R}_{y_m y_m}$  are the covariance matrices over that subcarrier. LMMSE is the best linear estimator that minimizes  $\mathbb{E} \|\mathbf{h}_m - \hat{\mathbf{h}}_m\|_2^2$ , and the NN learns the linear weights  $\mathbf{Q}_m$  and  $\mathbf{b}_m$  to minimize the empirical average MSE given by  $1/K \sum_{k=1}^K \|\mathbf{h}_m^{(k)} - \hat{\mathbf{h}}_m^{(k)}\|_2^2$ , where  $K$  is the size of the dataset.

We subsequently apply convolutional layers on these initial estimates to further improve the estimation performance by exploiting the inherent correlations within the channel matrix across subcarriers as well as antennas. This is motivated by our previous observations showing strong local correlations in MIMO channel matrices, which explains the significant success of convolutional NNs in efficient MIMO CSI reduction and feedback [20], [23], [25]. To this end, we concatenate initial estimates from the dense branches to get  $\tilde{\mathbf{H}} = [\tilde{\mathbf{h}}_1, \dots, \tilde{\mathbf{h}}_M]$ , which is then input to the convolutional layers, as shown in Fig. 1. The convolutional layers exploit these spatial and inter-frequency correlations in the channel matrix to provide an accurate final estimate  $\hat{H}$ . In Fig. 1, “Conv|128|5x5|ReLU|Same” represents a convolutional layer with 128 kernels of size  $5 \times 5$  with rectified linear (ReLU) activation and “Same” padding technique. “| - -|” means that the last layer has no activation. The final estimate is given by  $\hat{\mathbf{H}} = \mathcal{CONV}(\tilde{\mathbf{H}}; \Theta)$ ,

where  $\mathcal{CONV}$  and  $\Theta$  denote the convolutional layers and their corresponding set of parameters.

Finally, the network is trained to minimize the end-to-end empirical MSE cost given by

$$\begin{aligned} \mathcal{C}(\mathbf{H}; \mathbf{P}_1, \dots, \mathbf{P}_M, \mathbf{Q}_1, \dots, \mathbf{Q}_M, \Theta) &= \frac{1}{K} \sum_{k=1}^K \text{MSE}(\mathbf{H}^{(k)}, \hat{\mathbf{H}}^{(k)}) \\ &= \frac{1}{K} \sum_{k=1}^K \|\mathbf{H}^{(k)} - \mathcal{CONV}(\tilde{\mathbf{H}}^{(k)}; \Theta)\|_2^2, \end{aligned} \quad (3)$$

where  $K$  is the size of the dataset. Minimizing (3) end-to-end, we obtain all the network parameters including the pilot signals  $\mathbf{P}_1, \dots, \mathbf{P}_M$ .

**Remark 1:** In comparison with the simple LMMSE estimate, our proposed NN-based approach is data-driven in the sense that, it does not make any prior assumption on channel statistics but rather learns them over the dataset during training. Although LMMSE is optimum when channel and noise distributions are jointly Gaussian, the general MMSE estimate  $\hat{\mathbf{H}} = \mathbb{E}[\mathbf{H}|\mathbf{Y}]$  has no closed-form expression for arbitrary channel distributions. Our proposed NN-based channel estimator is trained to minimize the empirical MSE, and hence, gives a tractable approximation of the general MMSE estimate. The Gaussian channel assumption is based on the central limit theorem, which requires the number of multi-path components to be large enough. Hence, in practice the channel distributions may deviate from Gaussian, which will degrade the LMMSE performance. Our proposed NN-based approach learns the MMSE estimate regardless of the channel distributions. We later show through simulations that our proposed NN-based approach outperforms LMMSE for short pilot lengths  $L$  and low SNR values.

**Remark 2:** There has been a prior line of research to analytically design optimum pilot signals for downlink FDD MIMO systems [26]–[28]. When the channel distribution is assumed to be Gaussian, the resulting MSE of the LMMSE estimator has a closed-form expression. The authors in [27] use steepest descent optimization to design pilots that minimize the resulting MSE. This approach again relies heavily on the Gaussian channel assumption. If this assumption is even slightly generalized to be a Gaussian mixture instead of a single Gaussian, then there only exists closed-form expressions for the upper and lower bounds on the MSE [28]. The authors in [28] use steepest descent to design pilots that maximize the mutual information between the received noisy pilots and the channel, i.e.,  $I(\mathbf{Y}; \mathbf{H})$ . Our NN approach, however, jointly designs channel estimator and pilot signals to minimize the end-to-end estimation error while avoiding computational difficulties.

**Remark 3:** The authors in [11], [24] utilize a CNN-based architecture for MIMO channel estimation, but they use simple FFT pilot signals. However, in this paper, we add the fully

connected reduction layers to the CNN architecture to jointly optimize pilots and estimate the channel. We show later in the ablation study that the designed pilot signals significantly improve the performance. They also use the CNN structure on an initial least square (LS) channel estimate to improve the estimation performance. We observed in simulations that replacing the initial LS estimate with the fully connected expansion layers lets the network to automatically learn the initial estimate and improves the end-to-end reconstruction MSE. Although the approach proposed in [11], [24], outperforms non-ideal LMMSE (where the covariance matrices are estimated from a coarse initial LS estimate at the user), it still performs worse than the ideal LMMSE. We later show through simulations that our proposed NN-based approach outperforms ideal LMMSE (where the covariance matrices are estimated over the dataset) for short pilot lengths  $L$  and low SNR values.

**Remark 4:** The authors in [10] use a similar NN structure, but they employ the same pilot signals over all the subcarriers. However, we observe different channel statistics over different subcarriers, which suggests that employing the same pilots over all the subcarriers is sub-optimal. In this work we use a frequency-aware pilot design approach, which utilizes different fully connected branches over different subcarriers to design pilots. We later show through simulations that our frequency-aware approach improves the MSE by a considerable margin. It also allows us to non-uniformly allocate pilots to different subcarriers, by our proposed NN pruning technique which further reduces the MSE with the same pilot overhead. Our proposed pruning-based pilot allocation approach is described in details in the following section.

#### IV. PILOT ALLOCATION BY NN PRUNING

In this section we propose an efficient pilot allocation technique by pruning least significant neurons from the fully connected layers in our proposed NN architecture. The reduction layer in the  $m$ 'th fully connected branch consists of  $L$  neurons each of which corresponds to a single pilot transmission according to  $\tilde{\mathbf{y}}_m = \mathcal{FC}_m^r(\mathbf{h}_m; \mathbf{P}_m) = \mathbf{P}_m \mathbf{h}_m$ , and occupies one time-frequency resource over the downlink channel. Denote the pilot matrix by  $\tilde{\mathbf{Y}} = [\tilde{\mathbf{y}}_1, \tilde{\mathbf{y}}_2, \dots, \tilde{\mathbf{y}}_M]$ , which represents a total of  $L \times M$  time-frequency resources allocated to downlink pilots during each coherence interval of the channel. Our idea is to gradually prune least significant neurons from the fully connected reduction layers  $\mathcal{FC}_1^r, \dots, \mathcal{FC}_M^r$  during training to reduce the pilot overhead by saving the corresponding time-frequency resources for data transmission, while causing the least possible degradation to the reconstruction MSE. This approach enables non-uniform pilot



allocation, allowing less pilot transmissions on subcarriers that can be satisfactorily reconstructed by the subsequent convolutional layers utilizing inter-frequency correlations.

Inspired by [29], we take a regularized magnitude-based pruning approach by introducing two modifications to the training process. Note that the  $(i, j)$ 'th pilot signal is given by

$$[\tilde{\mathbf{Y}}]_{ij} = [\tilde{\mathbf{y}}_j]_i = [\mathcal{F}\mathcal{C}_j^r(\mathbf{h}_j; \mathbf{P}_j)]_i = [\mathbf{P}_j \mathbf{h}_j]_i = \sum_{n=1}^N [\mathbf{P}_j]_{in} [\mathbf{h}_j]_n, \quad (4)$$

where  $[\cdot]_{ij}$  represents the  $(i, j)$ 'th element of a matrix. Define  $\Phi = [\Phi]_{ij} = \sum_{n=1}^N \|[\mathbf{P}_j]_{in}\|^2$ . Our idea is to prune neurons with the smallest sum squared weight connections (i.e., the smallest  $[\Phi]_{ij}$ ) from the network. With this in mind, we make the following modifications to the training process:

*Sparsity promoting regularization:* We add a second term to our cost function to push  $[\Phi]_{ij}$  elements towards zero, which then allows to prune neurons with smallest  $[\Phi]_{ij}$  values from the network by our subsequent magnitude-based pruning scheme. We add the  $l_1$ -norm of the  $\Phi$  matrix to the cost function with a regularization parameter  $\lambda$ , which controls the trade-off between sparsity and the MSE according to

$$\begin{aligned} \mathcal{C}_{prun}(\mathbf{H}; \mathbf{P}_1, \dots, \mathbf{P}_M, \mathbf{Q}_1, \dots, \mathbf{Q}_M, \Theta) &= \frac{1}{K} \sum_{k=1}^K MSE(\mathbf{H}^{(k)}, \hat{\mathbf{H}}^{(k)}) + \lambda \|\Phi\|_1 \\ &= \frac{1}{K} \sum_{k=1}^K \|\mathbf{H}^{(k)} - \hat{\mathbf{H}}^{(k)}\|_2^2 + \lambda \sum_i \sum_j \left| \sum_{n=1}^N \|[\mathbf{P}_j]_{in}\|^2 \right|, \end{aligned} \quad (5)$$

where the  $\lambda$  value is determined through numerical search until a desired sparsity level is achieved. Denoting our target sparsity level by  $S$ , which represents the percentage of the pruned neurons, a larger  $\lambda$  is required for larger  $S$  values.

*Magnitude-based pruning:* Define a pilot allocation mask  $\mathbf{M} \in [0, 1]^{L \times M}$ , in which the zeros represent the pruned pilots. Pruning is performed by element-wise multiplication of the pruning mask with the received pilot matrix during each optimization step, i.e.,  $\mathbf{Y} = \mathbf{M} \odot \tilde{\mathbf{Y}} + \mathbf{N}$ . We initialize  $\mathbf{M}$  from an all-one state and gradually update it during training according to a pruning schedule to achieve the final allocation mask  $\mathbf{M}^*$ . Our target sparsity  $S$  represents the ratio of zeros in the final mask  $\mathbf{M}^*$  over its size,  $L \times M$ . As our regularization term gradually pushes more and more of the  $[\Phi]_{ij}$  values towards zero along the training steps, the  $[\mathbf{M}]_{ij}$  values corresponding to the smallest  $[\Phi]_{ij}$ 's can be zeroed out. We use a linear pruning schedule where we apply 10 balanced updates on  $\mathbf{M}$  during training, each of which prunes another  $S/10$  of the pilots by zeroing out another  $S/10$  of the  $[\mathbf{M}]_{ij}$  elements corresponding to the smallest  $[\Phi]_{ij}$

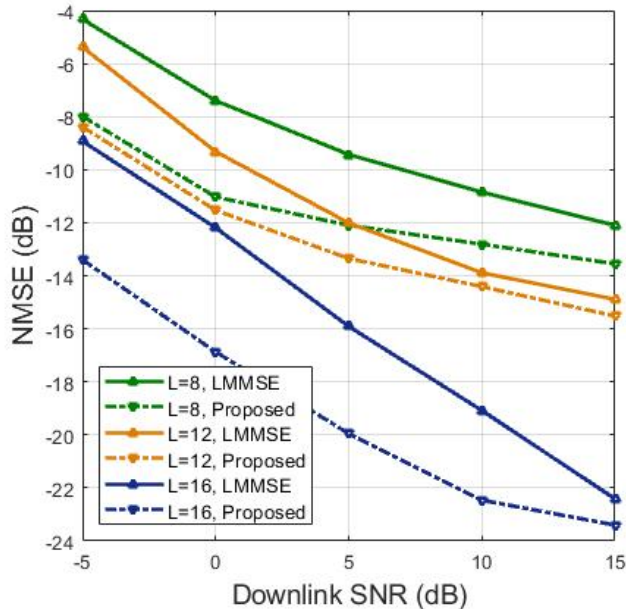


Fig. 2: NMSE (dB) vs. downlink SNR,  $N = 32$ ,  $M = 256$ .

values. It is important to train for sufficient number of steps after each update of the pruning mask to allow the network to converge to the new optimum before the next pruning update.

## V. SIMULATION RESULTS

We use the COST 2100 channel model [30] to generate datasets of channel matrices for training and testing our proposed network. We consider the indoor picocellular scenario at 5.3 GHz, where the BS is equipped with a ULA of dipole antennas positioned at the center of a  $20\text{m} \times 20\text{m}$  square. The user is placed within this square uniformly at random. All other parameters follow the default settings in [30]. Train and test datasets include 80000 and 20000 channel realizations, respectively, with  $M = 256$  and  $N = 32$ . We train all NNs up to 110000 steps and use the normalized MSE (NMSE) as the performance measure, defined by

$$\text{NMSE} \triangleq \frac{\mathbb{E}\{\|\mathbf{H} - \hat{\mathbf{H}}\|_2^2\}}{\mathbb{E}\{\|\mathbf{H}\|_2^2\}}. \quad (6)$$

### A. NN vs. LMMSE performance

Fig. 2 compares the NMSE for our proposed NN-based channel estimation technique with LMMSE for different pilot length and SNR values. Note that in this figure we have used the

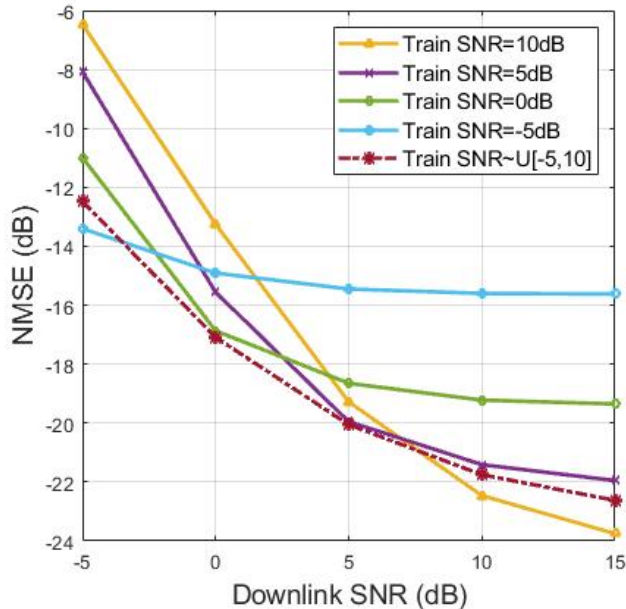


Fig. 3: NMSE (dB) vs. downlink SNR for the proposed scheme,  $L = 16$ ,  $N = 32$ ,  $M = 256$ .

pilot signals optimized by the fully connected reduction layers for both techniques. For LMMSE, we have first estimated the covariance matrices over the dataset and assumed the user has perfect knowledge of these covariance matrices. In practice, the user may estimate covariances from a coarse initial LS estimate, which degrades the LMMSE performance. Hence, the curves in Fig. 2 provide a lower bound on the performance of LMMSE as we have estimated the covariance matrices over the entire dataset.

According to Fig. 2, our proposed NN-based approach outperforms LMMSE for all SNR and pilot lengths. The improvement is particularly significant at low SNR regimes, e.g., our proposed NN-based approach improves the reconstruction NMSE by 3.66 dB at SNR=-5dB and  $L=8$ . Equivalently, for a target NMSE of -12dB at a downlink SNR of 5dB, our proposed NN-based approach reduces the required pilot length from 12 to 8 which is a 33.3% reduction in the pilot overhead.

### B. Frequency-aware improvements

Unlike [10] which optimizes the same pilots over all subcarriers, our proposed NN architecture utilizes  $M$  parallel fully connected branches to design different pilots over subcarriers. This helps to improve the NMSE performance by allowing the NN to learn and exploit specific subcarrier

TABLE I: Comparison of the NMSE (dB) achieved using same pilots (SP) over all subcarriers [10] and the proposed frequency-aware pilot design scheme (DP) for  $N = 32$ ,  $M = 256$ .

SNR		-5 dB	0 dB	5 dB	10 dB	15 dB	20 dB
L=16	DP	-13.40	-16.87	-19.95	-22.46	-23.40	-23.75
	SP	-11.84	-15.07	-18.08	-20.58	-22.34	-23.25
L=12	DP	-8.39	-11.53	-13.35	-14.41	-15.52	-16.40
	SP	-7.92	-10.92	-11.74	-12.91	-13.30	-13.94
L=8	DP	-7.99	-11.03	-12.10	-12.87	-13.55	-14.05
	SP	-7.74	-9.38	-10.69	-12.12	-12.99	-13.42

statistics and structures in a frequency-aware manner. Table I provides a comparison between our proposed frequency-aware pilot design scheme with the approach proposed in [10], where the same pilots are used over different subcarriers. The acronyms “DP” and “SP” in this table represent “different pilots” and “same pilots” approaches, respectively. According to Table I, our proposed frequency-aware approach improves the performance significantly, e.g. for a target NMSE of  $-12.9$ dB at a downlink SNR of 10dB, our proposed approach reduces the required pilot length from 12 to 8 which is a 33.3% reduction in the pilot overhead. This shows the benefits of frequency-aware pilot design over subcarriers.

### C. Impact of channel SNR

Fig. 3 studies the performance of the proposed scheme when there is a mismatch between the downlink SNR and the SNR value used for training. This figure plots the NMSE versus SNR curves for networks trained with each specific SNR value. We see that the NMSE degrades when the downlink SNR falls below the SNR value used for training. On the other hand, for a network trained with a lower SNR value, the performance saturates when downlink SNR improves above the training SNR. The dashed curve represents the performance of a NN trained over a dataset with sample SNRs picked uniformly at random from the interval  $[-5, 10]$ dB. As observed in this figure, such a NN performs satisfactorily over the whole SNR range.

### D. Ablation study

To study the improvements by each component of our proposed NN architecture, we provide ablation results in Table II. We compare 4 different schemes as below:

TABLE II: Ablation results of NMSE (dB) for  $L = 16$ ,  $N = 32$ ,  $M = 256$ .

SNR	-5dB	0dB	5dB	10dB	15dB	20dB
Proposed (NN+NN)	-13.40	-16.87	-19.95	-22.46	-23.40	-23.75
NN+LMMSE	-9.24	-12.45	-16.17	-19.83	-22.76	-24.41
FFT+NN	-7.22	-8.25	-13.22	-14.09	-15.70	-16.26
FFT+LMMSE	-0.86	-0.92	-1.19	-1.77	-2.77	-4.17

- Our proposed scheme, in which both the pilot design and channel estimation are handled by the NN. This scheme is denoted by “NN+NN” in the table.
- A scheme, which uses LMMSE for channel estimation while the pilots are designed using a NN. In this case we take the received pilot vectors  $\mathbf{y}_m = \mathbf{P}_m^* \mathbf{h}_m + \mathbf{n}_m$  from the fully connected branches and apply ideal LMMSE (utilizing covariances estimated over the dataset) on it, where  $\mathbf{P}_m^*$  denotes the pilots optimized by the NN. This scheme is denoted by “NN+LMMSE” in the table.
- A scheme that employs a NN for channel estimation, but simple FFT pilots are used similarly to [24] and [11]. Note that, in this scheme, we retrain the NN replacing  $\mathbf{P}_m$ 's with a submatrix of DFT. This scheme is denoted by “FFT+NN” in the table.
- The conventional scheme using FFT pilots and LMMSE estimation. This scheme is denoted by “FFT+LMMSE” in the table.

According to Table II, our proposed all NN-based scheme outperforms significantly all three schemes, with the NN-based pilot design leading to a remarkable improvement in the reconstruction NMSE. The conventional FFT+LMMSE scheme performs poorly at all channel SNRs as channel estimation is severely underdetermined for  $N = 32$  and  $L = 16$ .

### E. Pilot pruning

Table III provides a summary of the results obtained by our proposed pilot pruning scheme. In particular, we present the NMSE as a function of the sparsity level for different pilot lengths when SNR=10dB,  $N = 32$  and  $M = 256$ . The numbers in parentheses show the  $\lambda$  values used to achieve the sparsity level in each simulation according to Eq. (5). We observe that the same  $\lambda$  value performs fairly well for a number of settings, e.g., we get good results with  $\lambda = 10^{-6}$  for all  $S \leq 50\%$  for  $L = 8$  and 12. We observed that a well-performing  $\lambda$  value can always be found by trying only a few negative exponents of 10, i.e.,  $\{10^{-3}, 10^{-4}, 10^{-5}, 10^{-6}\}$ .

TABLE III: NMSE (dB) performance achieved for different sparsity levels by the pruning-based pilot reduction technique at SNR=10dB,  $N = 32$ ,  $M = 256$ . Values of  $\lambda$  (in Eq. (5)) to achieve the specified sparsity level are given in parentheses.

	$S = 0\%$	$S = 5\%$	$S = 10\%$	$S = 15\%$	$S = 20\%$	$S = 25\%$
$L = 16$	-22.46	-20.73 ( $10^{-6}$ )	-19.68 ( $10^{-5}$ )	-19.45 ( $10^{-5}$ )	-19.23 ( $10^{-5}$ )	-19.06 ( $10^{-5}$ )
$L = 12$ ( $10^{-6}$ )	-14.41	-13.69	-13.71	-13.52	-13.47	-13.33
$L = 8$ ( $10^{-6}$ )	-12.81	-12.36	-11.96	-11.86	-11.78	-11.52

TABLE IV: Pilot allocation performance by NN pruning at SNR=10dB,  $N = 32$ ,  $M = 256$ .

	$L = 6, S = 0\%$	$L = 8, S = 25\%$	$L = 12, S = 50\%$
NMSE (dB)	-10.38	-11.52 ( $10^{-6}$ )	-12.42 ( $10^{-6}$ )

According to Table III, the NMSE value degrades slowly as we increase the sparsity; and hence, the proposed pruning scheme can be used to efficiently reduce the pilot overhead without significantly degrading the channel estimation accuracy. For example, when  $L = 12$ , our proposed pilot pruning scheme can save up to 25% of the time-frequency resources while degrading the NMSE by only 1.08dB. Note that the number of time-frequency resources occupied with pilots is the same for  $L = 16, S = 25\%$  and  $L = 12, S = 0\%$ , while the corresponding NMSE values are  $-19.06$ dB and  $-14.41$ dB for these two settings, respectively. Hence, our proposed pruning scheme can efficiently allocate pilots non-uniformly along subcarriers to improve the performance while using the same number of time-frequency resources.

To elaborate further, we train for the three settings in Table IV, all of which use  $6 \times 256 = 1536$  time-frequency resources for pilot transmission. According to this table, we can improve the NMSE by  $2.04$ dB, for the same pilot overhead, by starting from  $L = 12$  and pruning the network with our proposed scheme. Of course,  $L = 12$  increases the estimation delay at the receiver as the user cannot estimate the channel until all 12 pilots are received over some sub-carriers.

Table IV shows that when a fixed budget of time-frequency resources is available for pilot transmission, starting from a larger  $L$  value and pruning the network down to the available resource budget results in an improved NMSE performance. The NN achieves this by allocating less pilots to sub-carriers that can be sufficiently interpolated by the network exploiting the statistical CSI correlations while using more pilots on other subcarriers. Fig. 4 depicts the

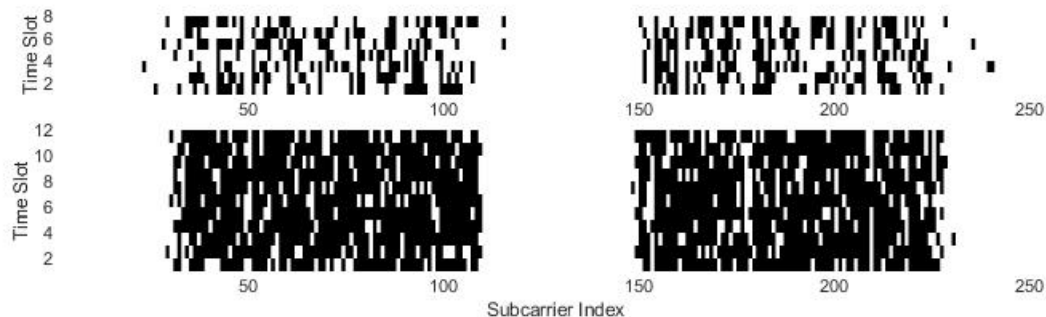


Fig. 4: Pilot allocation masks for the proposed NN pruning-based scheme.

resulting allocation masks  $M$  for (a)  $L = 8, S = 25\%$  and (b)  $L = 12, S = 50\%$ , where the white dots represent the time-frequency resources devoted to pilots, while the black dots represent those saved for data transmission. As observed in this figure, more resources can be saved for data over subcarriers in the ranges (30-110) and (150-230) in the setting considered.

## VI. CONCLUSION

We have proposed a NN-based joint downlink pilot design and channel estimation scheme for FDD massive MIMO-OFDM systems. Our proposed network utilizes dense layers to design pilot signals in a frequency-aware structure followed by convolutional layers which utilize inherent local correlations in the channel matrix to provide an accurate channel estimate. We also proposed an effective pilot reduction technique by gradually pruning less significant neurons from the dense layers to reduce the pilot overhead and to save time-frequency resources for data transmission. Our proposed NN-based scheme outperforms linear minimum mean square error (LMMSE) estimation. The proposed scheme learns the channel statistics over the training data and exploits it to estimate the channel in a data-driven manner without prior statistical assumptions on the channel distributions. Our pruning-based pilot reduction technique effectively reduces the pilot overhead by allocating pilots across subcarriers non-uniformly; allowing less pilot transmissions on subcarriers that can be satisfactorily reconstructed by the subsequent convolutional layers utilizing inter-frequency correlations.

## REFERENCES

- [1] X. Rao and V. K. N. Lau, "Distributed compressive CSIT estimation and feedback for FDD multi-user massive MIMO systems," *IEEE Transactions on Signal Processing*, vol. 62, no. 12, pp. 3261–3271, 2014.

- [2] Z. Gao, L. Dai, Z. Wang, and S. Chen, "Spatially common sparsity based adaptive channel estimation and feedback for FDD massive MIMO," *IEEE Transactions on Signal Processing*, vol. 63, no. 23, pp. 6169–6183, 2015.
- [3] Z. Gao, L. Dai, W. Dai, B. Shim, and Z. Wang, "Structured compressive sensing-based spatio-temporal joint channel estimation for FDD massive MIMO," *IEEE Transactions on Communications*, vol. 64, no. 2, pp. 601–617, 2016.
- [4] Y. Han, J. Lee, and D. J. Love, "Compressed sensing-aided downlink channel training for FDD massive MIMO systems," *IEEE Transactions on Communications*, vol. 65, no. 7, pp. 2852–2862, 2017.
- [5] X. Kuai, L. Chen, X. Yuan, and A. Liu, "Structured turbo compressed sensing for downlink massive MIMO-ofdm channel estimation," *IEEE Transactions on Wireless Communications*, vol. 18, no. 8, pp. 3813–3826, 2019.
- [6] J. Fang, X. Li, H. Li, and F. Gao, "Low-rank covariance-assisted downlink training and channel estimation for FDD massive MIMO systems," *IEEE Transactions on Wireless Communications*, vol. 16, no. 3, pp. 1935–1947, 2017.
- [7] X. Li, J. Fang, H. Li, and P. Wang, "Millimeter wave channel estimation via exploiting joint sparse and low-rank structures," *IEEE Transactions on Wireless Communications*, vol. 17, no. 2, pp. 1123–1133, Feb 2018.
- [8] M. B. Mashhadi and D. Gündüz, "Deep learning for massive MIMO channel state acquisition and feedback," *arXiv:2002.06945 [cs.IT]*, Feb. 2020.
- [9] Z. Liu, L. Zhang, and Z. Ding, "Overcoming the channel estimation barrier in massive MIMO communication systems," *arXiv:1912.10573 [cs.IT]*, Dec. 2019.
- [10] X. Ma and Z. Gao, "Data-driven deep learning to design pilot and channel estimator for massive MIMO," *IEEE Transactions on Vehicular Technology*, vol. 69, no. 5, pp. 5677–5682, 2020.
- [11] P. Dong, H. Zhang, G. Y. Li, I. S. Gaspar, and N. NaderiAlizadeh, "Deep CNN-based channel estimation for mmwave massive MIMO systems," *IEEE Journal of Selected Topics in Signal Processing*, vol. 13, no. 5, pp. 989–1000, Sep. 2019.
- [12] Y. Zhang, M. Alrabeiah, and A. Alkhateeb, "Deep learning for massive MIMO with 1-bit ADCs: When more antennas need fewer pilots," *arXiv: 1910.06960 [cs.IT]*, 2019.
- [13] E. Balevi and J. G. Andrews, "Two-stage learning for uplink channel estimation in one-bit massive MIMO," *arxiv: 1911.12461 [eess.SP]*, 2019.
- [14] S. Gao, P. Dong, Z. Pan, and G. Y. Li, "Deep learning based channel estimation for massive MIMO with mixed-resolution ADCs," *IEEE Communications Letters*, vol. 23, no. 11, pp. 1989–1993, Nov 2019.
- [15] H. He, C. Wen, S. Jin, and G. Y. Li, "Deep learning-based channel estimation for beamspace mmwave massive mimo systems," *IEEE Wireless Communications Letters*, vol. 7, no. 5, pp. 852–855, 2018.
- [16] C.-K. Wen, W.-T. Shih, and S. Jin, "Deep learning for massive MIMO CSI feedback," *IEEE Wireless Commun. Lett.*, vol. 7, no. 5, pp. 748–751, 2018.
- [17] T. Wang, C. Wen, S. Jin, and G. Y. Li, "Deep learning-based CSI feedback approach for time-varying massive MIMO channels," *IEEE Wireless Commun. Lett.*, vol. 8, no. 2, pp. 416–419, April 2019.
- [18] Z. Liu, L. Zhang, and Z. Ding, "Exploiting bi-directional channel reciprocity in deep learning for low rate massive MIMO CSI feedback," *IEEE Wireless Commun. Lett.*, pp. 1–1, 2019.
- [19] J. Guo, C. Wen, S. Jin, and G. Y. Li, "Convolutional neural network based multiple-rate compressive sensing for massive MIMO CSI feedback: Design, simulation, and analysis," *IEEE Transactions on Wireless Communications*, pp. 1–1, 2020.
- [20] Q. Yang, M. B. Mashhadi, and D. Gunduz, "Distributed deep convolutional compression for massive MIMO CSI feedback," *arXiv: 2003.04684 [eess.SP]*, 2020.
- [21] J. Guo, X. Yang, C.-K. Wen, S. Jin, and G. Y. Li, "DL-based CSI feedback and cooperative recovery in massive MIMO," *arXiv: 2003.03303 [cs.IT]*, 2020.
- [22] Y. Jang, G. Kong, M. Jung, S. Choi, and I. Kim, "Deep autoencoder based CSI feedback with feedback errors and feedback delay in FDD massive MIMO systems," *IEEE Wireless Commun. Lett.*, vol. 8, no. 3, pp. 833–836, June 2019.



- [23] M. B. Mashhadi, Q. Yang, and D. Gunduz, "CNN-based analog CSI feedback in FDD MIMO-OFDM systems," in *2020 IEEE 45th International Conference on Acoustics, Speech, and Signal Processing (ICASSP)*, 2020.
- [24] P. Dong, H. Zhang, G. Y. Li, N. NaderiAlizadeh, and I. S. Gaspar, "Deep cnn for wideband mmwave massive MIMO channel estimation using frequency correlation," in *ICASSP 2019 - 2019 IEEE International Conference on Acoustics, Speech and Signal Processing (ICASSP)*, 2019, pp. 4529–4533.
- [25] Q. Yang, M. B. Mashhadi, and D. Gunduz, "Deep convolutional compression for massive MIMO CSI feedback," in *2019 IEEE 29th International Workshop on Machine Learning for Signal Processing (MLSP)*, Oct 2019, pp. 1–6.
- [26] J. Fang, X. Li, H. Li, and F. Gao, "Low-rank covariance-assisted downlink training and channel estimation for FDD massive MIMO systems," *IEEE Transactions on Wireless Communications*, vol. 16, no. 3, pp. 1935–1947, 2017.
- [27] S. Bazzi and W. Xu, "Downlink training sequence design for FDD multiuser massive MIMO systems," *IEEE Transactions on Signal Processing*, vol. 65, no. 18, pp. 4732–4744, 2017.
- [28] Y. Gu and Y. D. Zhang, "Information-theoretic pilot design for downlink channel estimation in FDD massive MIMO systems," *IEEE Transactions on Signal Processing*, vol. 67, no. 9, pp. 2334–2346, 2019.
- [29] S. Han, J. Pool, J. Tran, and W. Dally, "Learning both weights and connections for efficient neural networks," in *Advances in Neural Information Processing Systems*, 2015, p. 11351143.
- [30] L. Liu, C. Oestges, J. Poutanen, K. Haneda, P. Vainikainen, F. Quitin, F. Tufvesson, and P. D. Doncker, "The COST 2100 MIMO channel model," *IEEE Wireless Commun.*, vol. 19, no. 6, pp. 92–99, December 2012.